ARTICLE

Synergistic Modification of PVC with Nitrogen-Containing Heterocycle and Tung-Oil Based Derivative for Enhanced Heat Stabilization and Plasticization Behavior

Mei Wang[1], Xinzhu Fan[1], Quan Bu[1], Puyou Jia[2,3,*] and Shouqi Yuan[4]

[1]School of Agricultural Engineering, Jiangsu University, Zhenjiang, 212013, China

[2]Institute of Chemical Industry of Forest Products, Chinese Academy of Forestry (CAF), Nanjing, 210042, China

[3]Key Laboratory of Chemistry and Engineering of Forest Products, State Ethnic Affairs Commission, Guangxi Key Laboratory of Chemistry and Engineering of Forest Products, Guangxi University for Nationalities, Nanning, 530006, China

[4]Research Center of Fluid Machinery Engineering and Technology, Jiangsu University, Zhenjiang, 212013, China

*Corresponding Author: Puyou Jia. Email: jiapuyou@icifp.cn

ABSTRACT

The additives present in polyvinyl chloride (PVC) materials are the major source of organic by-products during PVC degradation. The thermal stabilizer and plasticizer are the main additives that endow PVC with the required properties during its processing. However, these two additives easily migrate when samples are obtained by physical mixing of the additives with PVC. This causes the reduction of PVC sample efficacy and the increase in the formation of organic by-products in the radiolysis process. In this work, two kinds of grafted PVC samples (tung-oil derivative grafted PVC and Atz grafted PVC, abbreviated as P-GT$_4$ and P-AZ$_3$) were synthesized by chemical grafting of 3-amino-1,2,4-triazole (Atz) and tung-oil derivative on PVC, respectively. These two PVC samples were then blended at different mass ratios to obtain hybrid PVC materials with excellent plasticization, thermal stability and migration resistance ability. Differential scanning calorimetry (DSC), discoloration, Congo red test and thermogravimetric analysis (TGA) showed that when the mass ratio of P-GT$_4$ to P-AZ$_3$ in the mixed PVC resin was 1:3, the resulting P$_{1:3}$-GT$_4$-AZ$_3$ (P4) presented the best plasticization and thermal stability. The kinetics of thermal decomposition showed that the activation energy of P4 was much higher than that of the reference material [PVC/DOTP/CaSt$_2$/ZnSt$_2$, PVC/CZ41 for short] at mass loss $\alpha = 20\%$ and 80%. In addition, the leaching test showed that P4 material possessed excellent migration resistance ability.

KEYWORDS

Polyvinyl chloride; synergistic self-stabilization; internal plasticization; 3-amino-1,2,4-triazole; tung-oil derivative

Nomenclature

| Term 1 | Interpretation 1 |
| Term 2 | Interpretation 2 |

e.g.

| $\varnothing$ | Porosity |
| s | Skin factor |

1 Introduction

Polyvinyl chloride (PVC), as one of the five general plastics, is widely used in various fields of modern society [1,2]. Although PVC products maintain a long service life compared with other plastics, they eventually become PVC solid waste [3–5]. In recent years, the by-products produced in the process of PVC waste treatment have attracted wide attention [6]. Some of the by-products result from the PVC chain degradation, while others mainly come from the degradation of additives in PVC [7,8]. Additives contained in PVC materials, such as thermal stabilizers, plasticizers, etc. [9,10], give PVC materials the required properties and improve their stability during molding and utilization [11,12]. According to previous reports, plasticizers and thermal stabilizers are the main sources of organic by-products [13,14]. The thermal stabilizer, plasticizer and PVC are physically blended during the processing of commercial PVC materials [15–17]. However, the poor compatibility of PVC and additives easily leads to the uneven dispersion of additives and the migration of organic functional components, which results in the decrease in PVC sample efficiency and the increase in the formation of organic by-products during radiolysis [1,18]. Grafting modification of PVC has been regarded as an effective technique to reduce the migration of additives. Therefore, it is of great significance to develop a non-toxic, environment-friendly, migration resistant and dispersive organic compound and graft it into PVC. This strategy cannot only improve the thermal stability, plasticization and migration resistance of PVC materials, but can also avoid additives from becoming the main source of organic by-products in PVC decomposition.

The use of internal plasticizer involves covalent bonding of plasticizer molecule to PVC polymer, making it a part of PVC molecule, which is an effective way to solve the migration of plasticizer molecule in PVC material [19,20]. According to previous studies, the introduction of oil derivatives containing flexible long carbon chains into PVC can significantly improve the plasticization and migration resistance of internally plasticized PVC material [19,21,22]. For example, Jia et al. prepared a series of internally plasticized PVC materials containing flexible long carbon chains from castor oil and soybean oil derivative [19]. However, the existing plasticized PVC materials are mainly used for the study of plasticization, and their initial and long-term thermal stabilities are not satisfactory. Therefore, it is necessary to improve the thermal stability of PVC materials while also improving the plasticization property. The introduction of new biomass-based derivatives with special thermally stable functional groups and flexible long carbon chains into the PVC chains via covalent bonds is a promising choice for constructing self-stabilized, self-plasticized and flexible PVC polymers. Wang et al. attached Mannich base derived from laurene to PVC through covalent bonding, and successfully developed a PVC material with both internal plasticization and internal thermal stability [23]. However, compared with commercial PVC samples, the initial and long-term thermal stabilities of the prepared PVC materials were not significantly improved.

It is found that the initial color, as well as the long-term thermal stability, can be significantly improved by the introduction of nitrogen-containing functional groups into PVC. For example, Wang et al. observed that the thermal stability of PVC was greatly enhanced when nitrogen-rich group-containing tung-oil-based Ca/Zn salts and polyol were utilized as thermal stabilizers [24]. Due to its high nitrogen content, Atz has a high absorption ability for hydrogen chloride, and is used to synthesize two-dimensional layered complex [Zn(ttr)(OAc)] [25,26]. When [Zn(ttr)(OAc)] was used as the thermal stabilizer, the thermal stability of the resulting PVC product was significantly improved [23]. Similarly, covalent grafting of Atz onto PVC structure can help construct self-stabilized PVC polymer. If Atz and fat derivatives containing long flexible carbon chains are introduced into PVC through chemical grafting, it is expected that PVC material with excellent thermal stability and plasticization can be obtained [27].

Therefore, in this paper, Atz and tung-oil derivatives were respectively introduced into PVC by chemical grafting to obtain two resins, which were then mixed in different proportions to prepare hybrid PVC materials. The experimental results showed that the obtained PVC materials presented good thermal stability, plasticization, and mechanical properties.

2 Experimental Section

2.1 Materials

3-amino-1,2,4-triazole (Atz, 96%, Aladdin, Shanghai, China), 3-aminopropyltriethoxysilane (APTES, 99%, Aladdin), N,N-dimethyl-formamide (DMF, 99%, Nanjing Chemical Reagent, China), methanol (99.5%, Aladdin), methanol (99.5%, Aladdin), tetrahydrofuran (THF, 99%, Nanjing Chemical Reagent), n-hexane (97%, Aladdin), CaSt$_2$ (6.59% Ca, Shandong Huikeo, China) and ZnSt$_2$ (10.28% Zn, Shandong Huike, China), polyvinyl chloride (PVC, S-1000, Shandong Qilu, China), di (2-ethylhexyl) terephthalate (DOTP, 98%, Aladdin), and dioctylphthalate (DOP, 99%, Aladdin) were used as received. A detailed description of the synthesis of GEHTMA-4 can be found in our previous study [28]. The synthesis route of GEHTMA-4 is depicted in Fig. S1.

2.2 Synthesis

2.2.1 Synthesis of P-GT$_g$

PVC, APTES and DMF (80 mL) were placed in a flask and maintained at 85°C for 4 h to obtain a yellowish viscous solution. Then GEHTMA was slowly dropped into the above solution and reacted at 85°C for 8 h. Finally, the resulting product was washed with 10 wt% methanol aqueous solution several times and dried in an oven at 60°C for 48 h to obtain a yellowish transparent flake solid P-GT$_g$. The synthetic route of P-GT$_g$ is shown in Fig. 1. All P-GT$_g$ (g = 2, 3 and 4) were prepared by the above method, and the reaction material ratio of PVC, APTES and GEHTMA are displayed in Table 1.
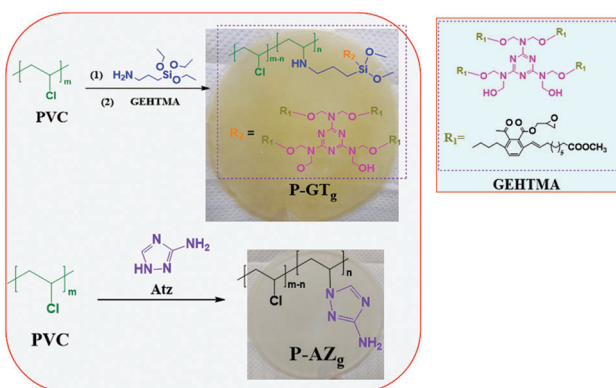
Figure 1: Synthesis routes of P-GT$_g$ and P-AZ$_g$

Table 1: The formulation for the synthesis of P-GT$_g$

Ingredients	Formulations/g		
	P-GT$_2$	P-GT$_3$	P-GT$_4$
PVC	5.0000	5.0000	5.0000
APTES	0.1966	0.2949	0.3932
GEHTMA	1.8443	2.7664	3.6885

2.2.2 Synthesis of P-AZ$_g$

PVC, Atz and DMF (100 ml) were placed in a flask and reacted at 85°C for 4 h to obtain a white viscous solution. Then the viscous solution was washed with 10 wt% methanol aqueous solution for several times

and dried in an oven at 60°C for 24 h to obtain a white transparent flake solid (P-AZ$_g$). All P-AZ$_g$ (g = 1, 2, 3) were synthesized at the same reaction conditions, and the mass ratio of PVC to Atz was 5:1, 5:2, and 5:3. The synthetic route of P-AZ$_g$ is shown in Fig. 1.

2.3 P-GT$_g$/P-AZ$_g$ Composite Film Preparation

P-GT$_g$, P-AZ$_g$ and THF (80 ml) were placed in a three-neck flask and held at 65°C for 4 h to obtain a viscous solution. The obtained solution was slowly put into a Petri dish, which was then dried in an oven at room temperature for 48 h to obtain P-GT$_g$/P-AZ$_g$ film. For comparison, PVC/CZ$_{41}$ obtained by an open mill was selected as the reference sample. 25 g PVC, 12.5 g DOTP, 0.75 g thermal stabilizers were milled into a homogeneous film using an open mill (ZG-50DR, Dongwan Province Xihua Testing Machines Co., Ltd., China) at 165°C for 5 min.

2.4 Characterization and Analysis

Fourier transform infrared (FT-IR) spectra, ^{1}H nuclear magnetic resonance (^{1}H NMR), gel permeation chromatography (GPC), differential scanning calorimetry (DSC), discoloration and congo red test, thermogravimetric analysis (TGA), thermal decomposition kinetics, Mechanical property and solvent resistance were investigated, and the comprehensive methods were provided in the Supplementary data.

3 Results and Discussion

3.1 Synthesis and Characterization

FT-IR spectra were obtained to identify the functional group changes of PVC before and after the modification with GEHTMA and APTES, as shown in Fig. 2a. The characteristic absorption bands at 3013, 1741, 1553, 1497, (910, 849, and 734) and 962 cm^{-1} are attributed to the vibration of C=C, C=O, triazine ring, epoxy group, and Si-O, respectively. It is found that all the P-GT$_g$ samples present these characteristic absorption bands, suggesting that the C=C, C=O, triazine ring, and epoxy groups of GEHTMA and Si-O of APTES are well retained after the incorporation of GEHTMA and APTES into PVC. The characteristic absorption bands at 962 and 617 cm^{-1} are attributed to the vibration of Si-O and C-Cl. The C-Cl absorption band at 617 cm^{-1} becomes weaker gradually as the chlorine atom is increasingly replaced, which indicates that the P-GT$_g$ samples are successfully obtained. ^{1}H NMR spectra of P-GT$_g$ samples were obtained to further verify their chemical structures (Fig. 2b). P-GT$_1$ presents several new peaks between 6.5-5 ppm (peaks 1, 2, 7, 8 and 23–28) and 3-1 ppm (peaks 21, 22, 29–31) compared with pure PVC. These peaks are assigned to the protons in −CH−C$\underline{H}$=C$\underline{H}$−CH−, −CH −C$\underline{H}$=C$\underline{H}$−CH$_2$, −N−C$\underline{H}_2$−O−, −C$\underline{H}_2$−O−C$\underline{H}_2$−, and −Si−O− C$\underline{H}_2$−C$\underline{H}_2$−C$\underline{H}_2$− NH−, respectively. The other characteristic peaks for P-GT$_g$ such as −C$\underline{H}_2$−C$\underline{H}_2$(Cl)−CH$_2$ (peak 1′ and peak 2′) are well maintained. The FT-IR and ^{1}H NMR results demonstrate that P-GT$_g$ was successfully synthesized.

The FT-IR spectra of P-AZ$_g$ materials are displayed in Fig. 2c. In the spectrum of Atz, the absorption bands located at 3419 and 3327 are attributed to the stretching vibration of the amino group, and the absorption band at 1640 cm^{-1} is assigned to the C=N bond of triazole in Atz. The intense absorption band of PVC located at 608 cm^{-1} is assigned to the absorption band of C-Cl. In the final product, the absorption band at 1638 cm^{-1} belonging to triazole (C=N) is retained. However, the absorption bands of the amino group at 3419 and 3327 cm^{-1} shift to 3411 and 3322 cm^{-1}, suggesting that the chemical environment of the amino group in Atz is changed. In addition, the peak at 608 cm^{-1} decreases in intensity with increasing replacement of chlorine atoms, suggesting the successful preparation of P-AZ$_g$. ^{1}H NMR was utilized to further investigate the chemical structure of P-AZ$_g$ (Fig. 2b). P-AZ$_1$ presents several new peaks (peaks 5 and 7) compared with pure PVC, which are assigned to the protons in –CH$_2$−C$\underline{H}$(N)−CH$_2$ and −N−C$\underline{H}$=N−. The other characteristic peaks for P-GT$_g$ such as −C$\underline{H}_2$−C$\underline{H}_2$(Cl) −CH$_2$ (peak 2), are well preserved. In addition, the chemical shift of –CH$_2$−C$\underline{H}$(Cl) (peak 3) at 3.76 ppm

shifts to 2.95 ppm, indicating the change in the chemical environment of $-CH_2-\underline{CH}(Cl)$. This phenomenon may originate from the replacement of the Cl atom in PVC by the amino group. The FT-IR and ^{1}H NMR results demonstrated that P-AZ$_g$ was successfully synthesized.
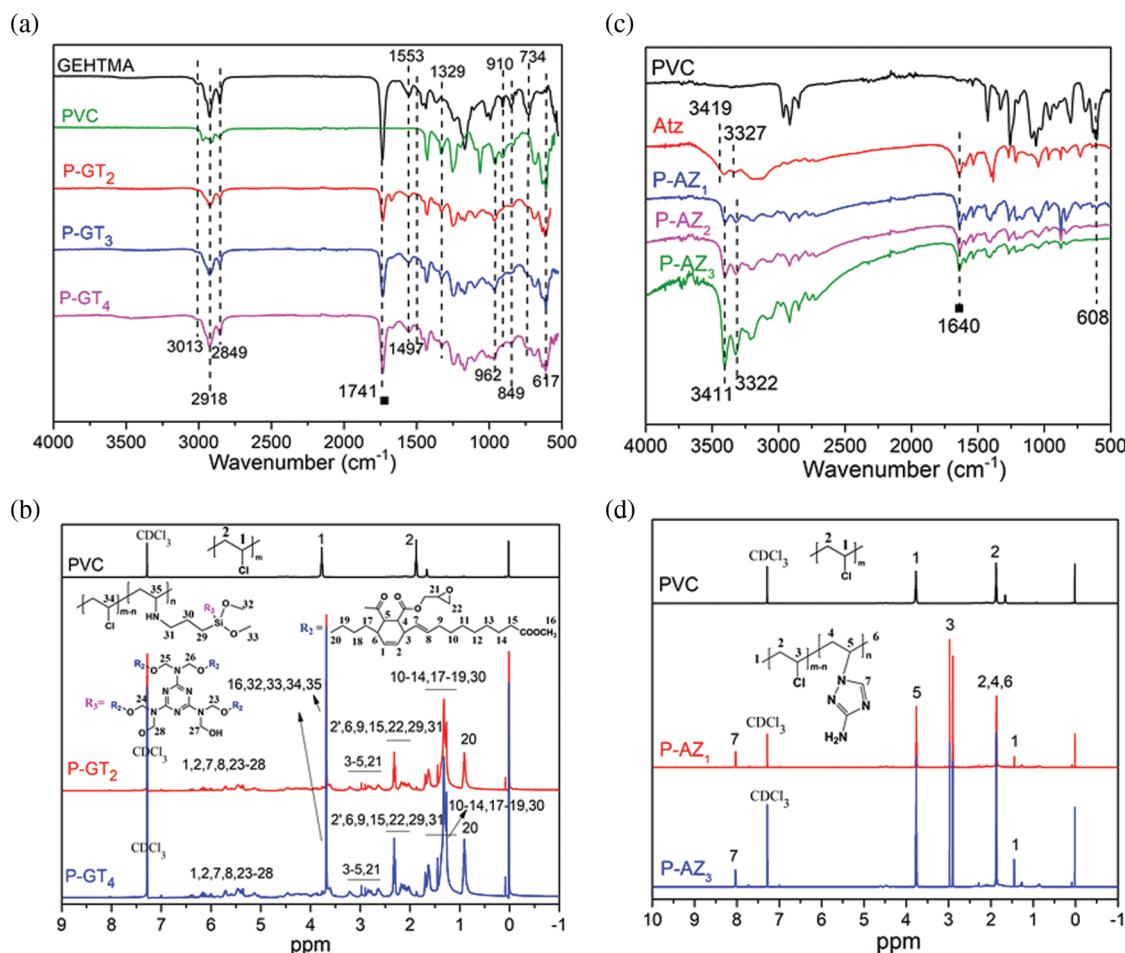

Figure 2: (a) FT-IR spectra of GEHTMA, PVC, and P-GT$_g$; (b) ^{1}H NMR spectra of PVC, and P-GT$_g$; (c) FT-IR spectra of PVC, Atz, P-AZ$_g$; (d) ^{1}H NMR spectra of PVC, and P-AZ$_g$

According to previous reports, the molecular weight change of PVC materials can serve as an indicator of the reaction between PVC and substituent [20]. Hence, GPC was used to study the average molecular weight and molecular weight distribution of PVC materials to obtain insight into the reaction of PVC. The GPC chromatograms of pure PVC, P-AZ$_g$ and P-GT$_g$ are shown in Fig. S2. The data of number average molecular weight (M_n), weight average molecular weight (M_w) and dispersity are shown in Table S1. It was found that the M_n and M_w changed with the replacement of chlorine atoms in PVC by the substitutes. The M_n and M_w of P-AZ$_g$ increased to 85738 and 180122 g/mol from 70738 and 153004 g/mol of PVC, respectively. Moreover, the M_n and M_w of P-GT$_g$ reached 90183 and 210187 g/mol, respectively, indicating the successful reaction of PVC with the substituent. In addition, compared with pure PVC, all P-AZ$_g$ and P-GT$_g$ samples showed a single chromatographic signal peak, which moved to a higher molecular weight region, indicating that the coupling reaction was not contaminated by homo-polymer [29].

3.2 Plasticizing Behavior of P-GT$_g$

Improving the plasticization can endow PVC with the desired properties, such as processability and flexibility, during processing. T_g was obtained by differential scanning calorimetry (DSC) and used to evaluate the plasticization efficiency of the plasticizer towards PVC. The free volume theory, a widely accepted plasticization theory, dictates that the polymer molecules are tightly packed and the free volume is small in the glassy state. Therefore, the polymer molecules cannot easily move in this state, presenting rigid and hard properties [30]. In the presence of the plasticizer, the distance between polymer molecules can be increased, and the free volume of the system increases as well, which leads to a reduction of viscosity and T_g of the polymer, and the increase in plasticization [22,31]. Fig. 3a shows that all grafted PVC materials displayed only one T_g, indicating their homogeneity. With the increase in grafting amount, the T_g of P-GT$_g$ decreased. In comparison to pure PVC and PVC/DOP (10:4 mass ratio of PVC/DOP), the T_g of P-GT$_4$ (with 45% grafting amount) was as low as 35.7°C. This phenomenon can be attributed to the increased free volume of the system, resulting from the irregular branched structure and the highly mobile terminal alkyl chain of grafted PVC. In view of the optimal plasticizing performance of P-GT$_4$, it was selected as the research object to further optimize its thermal stability.
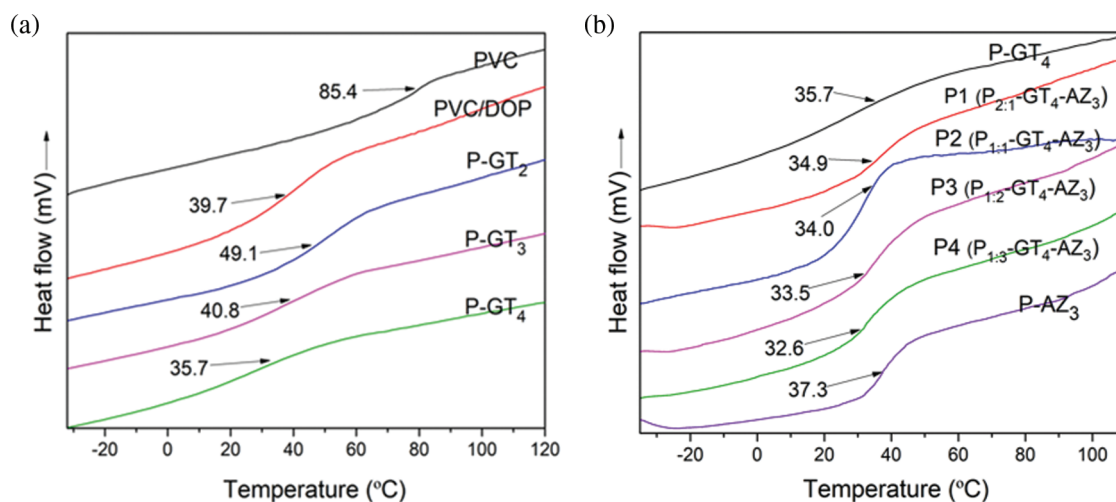
Figure 3: (a) DSC curves of PVC, PVC/DOP, P-GT$_g$ samples; (b) DSC curves of P-GT$_4$, P1, P2, P3, P4 and P-AZ$_3$ samples

3.3 Performance Evaluation of P-GT$_g$/P-AZ$_g$

3.3.1 Thermal Stabilizing Behavior Evaluated by Congo Red Test and Discoloration

As an important criterion for assessing PVC materials, thermal stability is closely related to the processability, mechanical properties and weather resistance of PVC. The unstable chlorine atoms in PVC readily leave under high temperatures, which leads to the release of hydrogen chloride as well as the formation of conjugated polyene [32]. With the increase in length of the conjugated polyene segment, the sample changes from colorless to yellow, orange, brown, and finally black [33]. Under the same conditions, PVC samples with better thermal stability show slower color change. The color change of PVC samples during thermal degradation at high temperatures can be obtained according to the oven method, and the results are shown in Table 2. The time taken for Congo red paper to turn blue after absorbing acid product is called T_s [11]. Therefore, hydrogen chloride and other acid products released at a high temperature can be determined by Congo red method, and the results are shown in Fig. 4. From Fig. 4 and Table 2, it was found that the above P-GT$_4$ with excellent plasticization presented good initial

thermal stability and long-term thermal stability at the same time. This result is because of the synergistic thermal stabilization effect of the triazine ring, hydroxyl group and epoxy functional group in P-GT$_4$ [24]. Compared with PVC/CZ41, the initial and long-term thermal stabilities of P-GT$_4$ were not satisfactory, and it turned completely black within 30 min due to "zinc burning". The high molecular weight of P-GT$_4$ decreased the unit molar weight of thermally stable functional groups. In addition, though the heat-stable functional groups in P-GT$_4$ can synergistically absorb HCl, they cannot effectively replace the Cl atom of PVC. Hence, the initial degradation and coloring cannot be inhibited efficiently.

Table 2: Color changes of grafted PVC samples during thermal aging in air

Different PVC samples	Thermal aging time (min)					
	0	10	20	30	40	50
PVC/CZ$_{41}$						
PVC						
P-GT$_4$						
P1(P$_{2:1}$-GT$_4$-AZ$_3$)						
P2(P$_{1:1}$-GT$_4$-AZ$_3$)						
P3(P$_{1:2}$-GT$_4$-AZ$_3$)						
P4(P$_{1:3}$-GT$_4$-AZ$_3$)						
P-AZ$_3$						
P-AZ$_2$						
P-AZ$_1$						
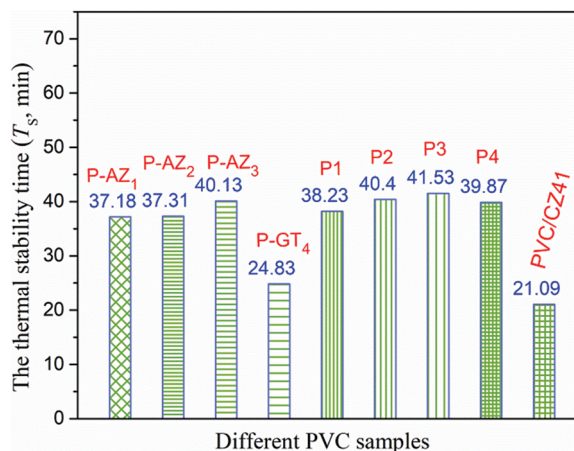
Figure 4: T_s value of different PVC samples

If an organic thermal stabilizer that can simultaneously absorb HCl and replace Cl atom in PVC chain is introduced into PVC sample, and then blended with P-GT$_4$, the resulting PVC material would be expected possess excellent plasticization and thermal stability. It is found that Atz can both absorb HCl and replace Cl atom on PVC chain, and can also eliminate the unstable structure causing heat degradation. The above factors are all favorable for inhibiting the initial degradation and coloring [23]. Congo red test (Fig. 4) and thermal aging (Table 2) were carried out to study the thermal stability of Atz grafted PVC (P-AZ$_1$, P-AZ$_2$ and P-AZ$_3$).

Compared with pure PVC and PVC/CZ41, the initial and long-term thermal stabilities of Atz grafted PVC were significantly improved, and further enhanced with the increase in Atz grafting amount in P-AZ$_g$, indicating that Atz grafted PVC possessed better thermal stability. In particular, the off-white P-AZ$_3$ displayed the maximum T_s value (40.13 min), and the "zinc burning" did not occur within 45 min, which indicates that P-AZ$_3$ had the best long-term thermal stability. P1, P2, P3 and P4 films were prepared by blending P-GT$_4$ and P-AZ$_3$ at the mass ratio of 2:1, 1:1, 1:2 and 1:3. It was found that with the increase in the amount of P-AZ$_3$ in P$_{g:g}$-GT$_4$-AZ$_3$ film, the T_s value first increased and then decreased, and the time of "zinc burning" of the samples gradually prolonged. Among them, P4 exhibited the best initial and long-term thermal stabilities, indicating that when the mass ratio of P-GT$_4$ to P-AZ$_3$ was 1:3, the synergistic thermal stability between the triazine ring, hydroxyl, epoxy functional groups and Atz was the best.

3.3.2 Thermal Stabilizing Behavior Evaluated by TGA Analysis

Thermogravimetric analysis (TGA) and DTG were carried out to evaluate the thermal stability of the prepared samples, and the results are displayed in Fig. 5. Clearly, all the samples presented two stages of sharp weight loss during the heating process. The first stage of weight loss within 200°C–300°C can be attributed to the degradation of the PVC main chain. In this process, the HCl molecule falls off from the PVC chain, leading to the formation of a conjugated polyene structure in PVC samples. The organic additives such as P-GT$_4$ and P-AZ$_3$ may also decompose at this temperature. The second stage of weight loss within 400°C–600°C likely results from the cyclization of conjugated polyene sequence, which leads to the formation of aromatic compounds [34]. Moreover, the carbonization of organic compounds at such a high temperature is also responsible for weight loss at this stage. The TGA curves of all the samples were analyzed in detail to obtain insight into the thermal stabilization behavior of the thermal stabilizers (Fig. 5a and Table 3). It was found that the initial thermal degradation temperature (T_{onset}) of P-AZ$_3$ was the highest among P-GT$_4$, P-AZ$_3$ and PVC/CZ$_{41}$, indicating the good initial thermal stability of P-AZ$_3$. However, P-AZ$_3$ presented poor performance compared with P-GT$_4$ and PVC/CZ$_{41}$ in terms of the temperature corresponding to 10% thermal weight loss (T_{10}) and the carbon residue rate at 250°C (W_{250}). With further increase in temperature, P-AZ$_3$ displayed a higher carbon residue rate at 350°C, 450°C and 598°C (W_{350}, W_{450}, W_{598}). The above phenomenon is related to the thermal stabilizer added to PVC samples. The heterocyclic Atz is more stable than the linear molecular structure of CaSt$_2$/ZnSt$_2$ and GEHTMA. Considering the merit of the synergistic effect, P-GT$_4$ was blended with P-AZ$_3$ to enhance its thermal stability. Interestingly, it was found that the resulting P3 and P4 showed a good synergistic effect and both displayed higher T_{onset}, T_{10}, W_{350}, W_{450}, and W_{598} compared with PVC/CZ$_{41}$, indicating better initial and long-term thermal stabilities of P3 and P4. The above results are in good agreement with Congo red and thermal aging test results.

3.3.3 Thermal Stabilizing Behavior Evaluated by Thermal Decomposition Kinetics Analysis

The thermal stability of PVC is related to its activation energy. Generally, during the thermal degradation process, the PVC samples with higher activation energy are more difficult to decompose, and the thermal stability is much higher [35]. TGA and DTG curves of P4 and PVC/CZ$_{41}$ at different heating rates were obtained by thermogravimetric analysis (Fig. 6). The detailed kinetic data are listed in Table S2. It can be seen from Fig. 6 that with the increase in heating rate, the T_{10}, T_{onset} and W_{598} of the polymer increased. The activation energy of all PVC materials (E_α, α = 20% and 80%) can be calculated by the Doyle equation, and the obtained results are shown in Fig. 7. At the mass loss of 20% and 80%, the E_α values of PVC/CZ$_{41}$ and P4 were 56.07, 79.19 and 126.52, 149.09, respectively. The activation energy of P4 was superior to that of PVC/CZ$_{41}$, implying the better thermal stability of P4.
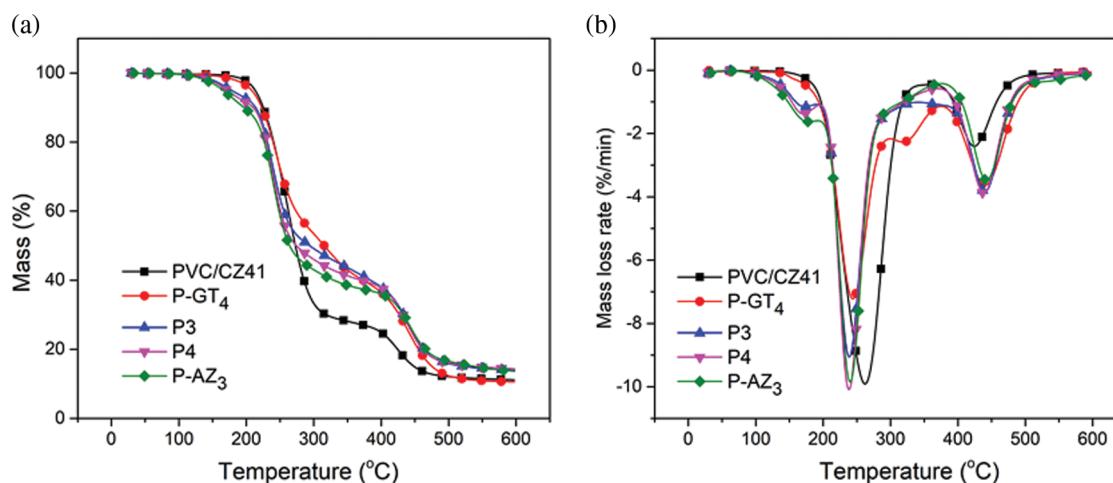
**Figure 5:** TGA (a) and DTG (b) curves of PVC samples

Table 3: Characteristic values from TGA and DTG curves

Samples	T_{onset} (°C)	T_{10} (°C)	W_{250} (%)	W_{350} (%)	W_{450} (%)	W_{598} (%)
PVC/CZ$_{41}$	219.92	225.16	71.99	28.11	14.88	11.15
P-GT$_4$	216.85	223.06	72.52	43.01	21.75	10.58
P3	220.43	213.89	63.74	43.65	23.60	13.87
P4	220.13	211.27	60.59	41.29	23.38	14.33
P-AZ$_3$	220.67	196.62	58.71	38.54	24.18	13.67

3.3.4 Plasticizing Behavior and Mechanical Properties of P-GT$_g$/P-AZ$_g$

P$_{g:g}$-GT$_4$-AZ$_3$ films (P1, P2, P3, P4) were prepared by blending P-GT$_4$ and P-AZ$_3$ at mass ratios of 2:1, 1:1, 1:2, and 1:3. The plasticizing properties of P-GT$_4$/P-AZ$_3$ were studied in depth, and the results are shown in Fig. 3b. All curves displayed only one T_g, indicating the homogeneity of the films obtained from blending of P-GT$_4$ and P-AZ$_3$. With the increase in P-AZ$_3$ content in P-GT$_4$/P-AZ$_3$ blended films, the T_g value first decreased and then increased. This phenomenon may result from the synergistic plasticization between P-AZ$_3$ with rigid nitrogen-containing five membered ring structures and P-GT$_4$ with flexible long carbon chains and numerous ester groups [21]. Among the P-GT$_4$/P-AZ$_3$ blended films, P4 presented the lowest T_g (32.6°C), which was far below that of pure PVC (85.4°C) and PVC/DOP (39.7°C). Hence, P4 showed excellent plasticization.

The mechanical properties of the samples were studied to further evaluate the plasticization of PVC and the results are shown in Fig. S3. It is well known that the internal molecular chemical structure, composition and crosslinking density are all responsible for the mechanical properties of PVC materials. P-GT$_4$ presented high tensile strength and elongation at break due to the existence of flexible long carbon chain, alicyclic structure, and triazine ring structure. With the increase in P-AZ$_3$ content in P-GT$_4$/P-AZ$_3$ blended films, the tensile strength increased gradually and the elongation at break increased first and then decreased. This was because the content of rigid triazole ring increased with the increase in P-AZ$_3$ content, so the strength and elongation at break also increased accordingly. P4 presented the best tensile strength as well as elongation at break.
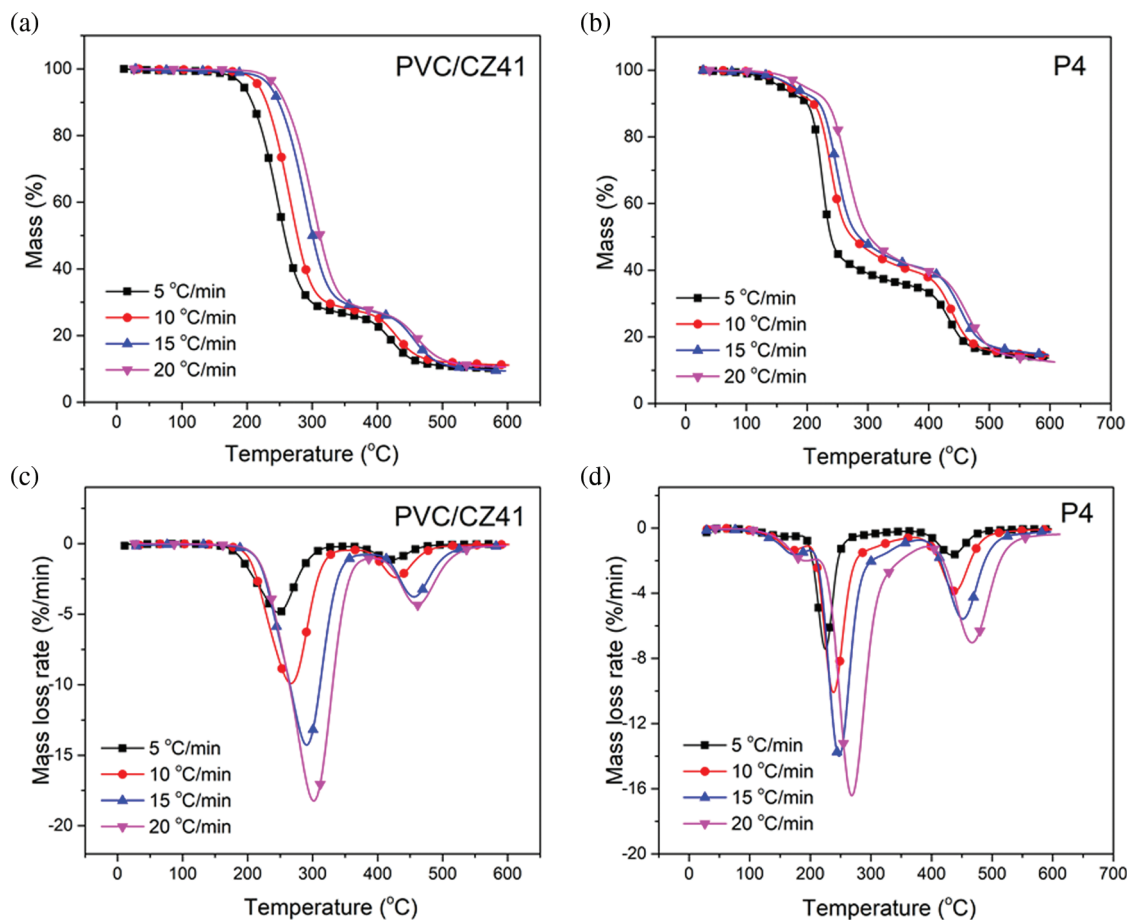
Figure 6: TGA (a–b) and DTG (c–d) curves of PVC/CZ$_{41}$ and P4 at various heating rates
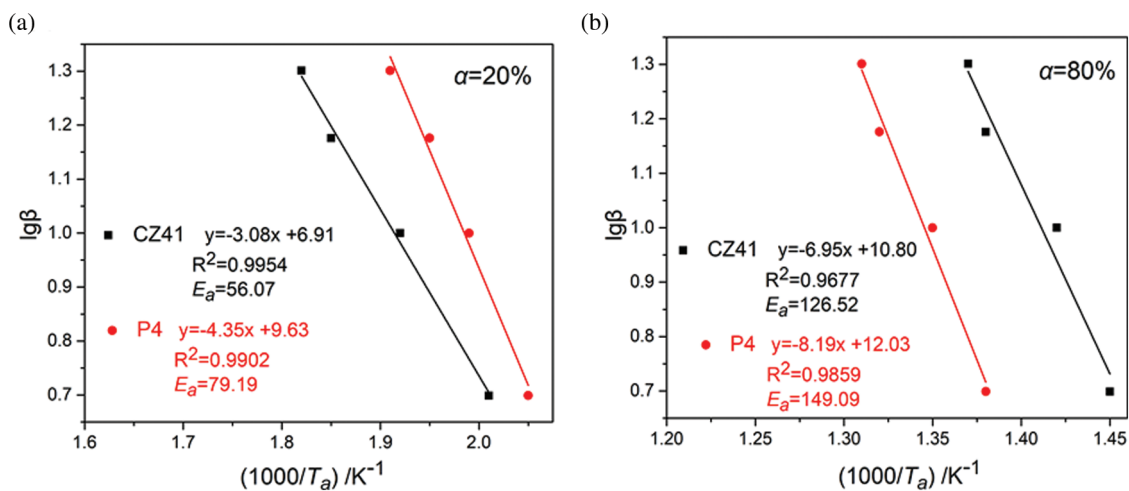
Figure 7: Linear plots of lgβ vs. (1000/T_α) based on Doyle equation

3.3.5 Migration Resistance Ability of P-GT$_g$/P-AZ$_g$

The migration resistance ability of PVC material was evaluated by a leaching test [36]. Fig. 8 shows the migration degree of various PVC materials in petroleum ether. The mobility values P-GT$_4$, P3, P4 and P-AZ$_3$ in petroleum ether were 1.78, 3.02, 1.11 and 3.46, respectively, which were much lower than that of PVC/CZ41 (27.75). Therefore, all the prepared grafted PVC samples showed excellent migration resistance ability.
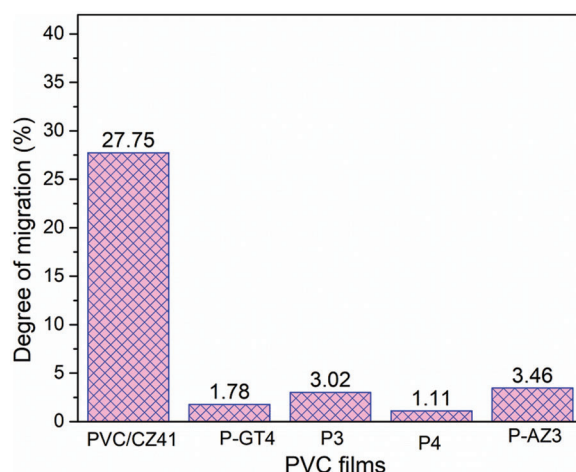
Figure 8: Weight loss after the leaching test for all PVC materials

4 Conclusion

In this paper, two kinds of grafted PVC materials (P-GT$_4$ and P-AZ$_3$) were synthesized by chemical grafting of Atz and tung-oil derivative onto PVC. Then, the two obtained grafted PVC materials were blended in different ratios to obtain a series of hybrid PVC materials with high thermal stability and good plasticization. The plasticization, thermal stability and migration stability of the materials were investigated in depth. When the mass ratio of P-GT$_4$ to P-AZ$_3$ in the mixed PVC resin was 1:3, the resulting P$_{1:3}$-GT$_4$-AZ$_3$ (P4) displayed the best performance with T_g of 32.6°C, T_s of 41.53 min, and the time of "zinc burning" delayed to 50 min. Compared with the reference PVC/CZ$_{41}$, P4 showed better plasticization, initial thermal stability and long-term thermal stability. The thermal decomposition kinetics results showed that at the mass loss of both 20% and 80%, the activation energy of P4 was higher than that of PVC/CZ$_{41}$, indicating its higher thermal stability. In addition, the leaching test showed that P4 material possessed excellent migration resistance ability. This study can serve as a reference for other researchers to develop synergistic modifications of PVC for enhanced heat stabilization and plasticization behavior.

Conflicts of Interest: The authors declare that they have no conflicts of interest to report regarding the present study.

References

1. Wang, Z., Xie, T., Ning, X. Y., Liu, Y. H., Wang, J. (2019). Thermal degradation kinetics study of polyvinyl chloride (PVC) sheath for new and aged cables. *Waste Management, 99,* 146–153. DOI 10.1016/j. wasman.2019.08.042.

2. Wang, C. J., Liu, H. R., Zhang, J. Q., Yang, S. L., Zhang, Z. et al. (2018). Thermal degradation of flame-retarded high-voltage cable sheath and insulation via TG-FTIR. *Journal of Analytical and Applied Pyrolysis, 134,* 167–175. DOI 10.1016/j.jaap.2018.06.005.

3. Miao, F., Liu, Y. F., Gao, M. M., Yu, X., Xiao, P. W. et al. (2020). Degradation of polyvinyl chloride microplastics via an electro-Fenton-like system with a TiO_2/graphite cathode. *Journal of Hazardous Materials, 399,* 123023. DOI 10.1016/j.jhazmat.2020.123023.

4. Nozue, K., Tagaya, H. (2021). Chemical recycling of waste Poly Vinyl Chloride (PVC) by the liquid-phase treatment. *Journal of Material Cycles and Waste Management, 23(2),* 489–504. DOI 10.1007/s10163-020-01153-9.

5. Han, W. Y., Zhang, M. Q., Kong, Y. F., Li, D. G., Liu, L. H. et al. (2020). Pentaerythritol stearate ester-based tin (II) metal alkoxides: A tri-functional organotin as poly (vinyl chloride) thermal stabilizers. *Polymer Degradation and Stability, 175,* 109129. DOI 10.1016/j.polymdegradstab.2020.109129.

6. Korpas, J., Slovák, V., Wichterle, K. (2016). Waste poly (vinyl chloride) pyrolysis with hydrogen chloride abatement by steelmaking dust. *Chemical Papers, 70(7),* 926–932. DOI 10.1515/chempap-2016-0025.

7. Lerke, I., Szymański, W. (1983). Stabilizationof gamma-irradiat ed poly(vinyl chloride) by epoxy compounds. II. Production of hydroperoxides in gamma-irradiated PVC-stabilizer mixtures. *Journal of Applied Polymer Science, 28(2),* 513–518. DOI 10.1002/app.1983.070280207.

8. Yu, J., Sun, L., Ma, C., Qiao, Y., Yao, H. (2016). Thermal degradation of PVC: A review. *Waste Management, 48,* 300–314. DOI 10.1016/j.wasman.2015.11.041.

9. Liu, D., Jiang, P., Nie, Z., Wang, H., Dai, Z. et al. (2020). Synthesis of an efficient bio-based plasticizer derived from waste cooking oil and its performance testing in PVC. *Polymer Testing, 90,* 106625. DOI 10.1016/j. polymertesting.2020.106625.

10. Thirupathiah, G., Satapathy, S., Palanisamy, A. (2019). Studies on epoxidised castor oil as co-plasticizer with epoxidised soyabean oil for PVC processing. *Journal of Renewable Materials, 7(8),* 775–785. DOI 10.32604/jrm.2019.06399.

11. Shariatmadari, R., Kalaee, M., Khajavi, R., Shariatinia, Z. (2021). Effect of zeolitic metal-organic framework on thermal, mechanical, and electrical properties of Ca/Zn-stabilized polyvinyl chloride. *Journal of Vinyl and Additive Technology, 27(18),* 1–11. DOI 10.1002/vnl.21822.

12. Sinyavsky, N., Korneva, I. (2017). Study of optical properties of polymeric materials subjected to degradation. *Journal of Polymers and the Environment, 25(4),* 1280–1287. DOI 10.1007/s10924-016-0908-y.

13. Yousif, E., Ahmed, D. S., Ahmed, A., Abdallh, M., Yusop, R. M. et al. (2019). Impact of stabilizer on the environmental behavior of PVC films reinforced 1,2,4-triazole moiety. *Environmental Science and Pollution Research, 26(25),* 26381–26388. DOI 10.1007/s11356-019-05784-w.

14. Chantreux, M., Ricard, D., Asia, L., Rossignol, S., Wong-Wah-Chung, P. (2021). Additives as a major source of radiolytic organic byproducts of polyvinyl chloride (PVC). *Radiation Physics and Chemistry, 188(26),* 109671. DOI 10.1016/j.radphyschem.2021.109671.

15. Pereira, V. A., Fonseca, A. C., Costa, C. S. M. F., Ramalho, A., Coelho, J. F. J. et al. (2020). End-capped biobased saturated polyesters as effective plasticizers for PVC. *Polymer Testing, 85,* 106406. DOI 10.1016/j. polymertesting.2020.106406.

16. Vassilev, D., Petkova, N., Koleva, M., Denev, P. (2018). Microwave synthesis of inulin acetate as potential bio-based additive for poly(vinyl chloride). *Journal of Renewable Materials, 6(7),* 707–714. DOI 10.32604/JRM.2018.00015.

17. Raeisi, A., Allahyari, F., Faghihi, K., Hosseini-Ghazvini, S. M., Khaleghi, M. et al. (2020). A complete description on effect of β-cyclodextrin-ester as a bio-based additive for preparation of safe PVC: From synthesis to computational study. *Materials Today Chemistry, 22(3),* 100736. DOI 10.1016/j.mtcomm.2019.100736.

18. Li, Q. G., Gong, S., Yan, J., Hu, H. C., Shu, X. G. et al. (2020). Synthesis and kinetics of hydrogenated rosin dodecyl ester as an environmentally friendly plasticizer. *Journal of Renewable Materials, 8(3),* 289–300. DOI 10.32604/jrm.2020.08897.

19. Navarro, R., Gacal, T., Ocakoglu, M., Garcia, C., Elvira, C. et al. (2017). Nonmigrating equivalent substitutes for PVC/DOP formulations as shown by a TG study of PVC with covalently bound PEO-PPO oligomers. *Macromolecular Rapid Communications, 38(6),* 1600734. DOI 10.1002/marc.201600734.

20. Navarro, R., Perrino, P. M., García, C., Elvira, C., Gallardo, A. et al. (2016). Highly flexible PVC materials without plasticizer migration as obtained by efficient one-pot procedure using trichlorotriazine chemistry. *Macromolecules, 49(6),* 2224–2227. DOI 10.1021/acs.macromol.6b00214.

21. Vahid, N., Hossein, A. (2020). Internally plasticized PVC by four different green plasticizer compounds. *European Polymer Journal, 128,* 109620. DOI 10.1016/j.eurpolymj.2020.109620.

22. Ma, Y. F., Liao, S. L., Li, Q. G., Guan, Q., Jia, P. Y. et al. (2020). Physical and chemical modifications of poly(vinyl chloride) materials to prevent plasticizer migration-still on the run. *Reactive & Function Polymers, 147(45),* 104458. DOI 10.1016/j.reactfunctpolym.2019.104458.

23. Wang, M., Wang, G. L., Song, X. H., Jia, P. Y., Zhou, B. L. et al. (2022). The thermal stabilization behavior and mechanism of a metal organic framework with high thermal stability towards PVC. *New Journal of Chemistry, 46(30),* 14395–14403. DOI 10.1039/D2NJ02233H.

24. Wang, M., Song, X. H., Jiang, J. C., Xia, J. L., Li, S. H. et al. (2017). Excellent hydroxyl and nitrogen rich groups-containing tung-oil-based Ca/Zn and polyol stabilizers for enhanced thermal stability of PVC. *Thermochimica Acta, 658,* 84–92. DOI 10.1016/j.tca.2017.10.008.

25. Ma, B., Wang, X., Lu, S. Y., He, H. W., Ma, M. et al. (2019). A novel double agent of triazole-based zinc-containing complex which constituted Zn/Zn stabilizer system with zinc stearate as thermal stabilizer for poly(vinyl chloride). *Polymer Degradation and Stability, 168(12),* 108953. DOI 10.1016/j.polymdegradstab.2019.108953.

26. Wang, X., Ma, B., Wang, Y. T., Lu, S. Y., Ma, M. et al. (2019). A new theory of two-step stabilization mechanism for triazole-based zinc-containing complex as thermal stabilizer for poly(vinyl chloride). *Polymer Degradation and Stability, 167(3),* 86–93. DOI 10.1016/j.polymdegradstab.2019.06.027.

27. Xia, Y., Huo, Y., Yang, Q., Zhou, H. M., Lin, X. J. et al. (2021). Study on preparation and properties of PVC/NBR/PVC-g-PMMA composite film. *Journal of Macromolecular Science, Part A, 58(9),* 636–641. DOI 10.1080/10601325.2021.1921597.

28. Wang, M., Song, X. H., Jiang, J. C., Xia, J. L., Ding, H. Y. et al. (2018). Plasticization and thermal behavior of hydroxyl and nitrogen rich group-containing tung-oil-based ester plasticizers for PVC. *New Journal of Chemistry, 42(4),* 2422–2431. DOI 10.1039/C7NJ03578K.

29. Jia, P. Y., Ma, Y. F., Song, F., Hu, Y., Zhang, C. Q. et al. (2019). Toxic phthalate-free and highly plasticized polyvinyl chloride materials from non-timber forest resources in plantation. *Reactive & Function Polymers, 144,* 104363. DOI 10.1016/j.reactfunctpolym.2019.104363.

30. Jie, C., Wang, Y. G., Huang, J. R., Li, K., Nie, X. A. (2018). Synthesis of tung-oil-based triglycidyl ester plasticizer and its effects on poly(vinyl chloride) soft films. *ACS Sustainable Chemistry & Engineering, 6(1),* 642–651. DOI 10.1021/acssuschemeng.7b02989.

31. Li, M., Li, S. H., Xia, J. L., Ding, C. X., Wang, M. et al. (2017). Tung oil based plasticizer and auxiliary stabilizer for poly(vinyl chloride). *Materials & Design, 122,* 366–375. DOI 10.1016/j.matdes.2017.03.025.

32. Gama, N., Santos, R., Godinho, B., Silva, R., Ferreira, A. (2019). Triacetin as a secondary PVC plasticizer. *Journal of Polymers and the Environment, 27(6),* 1294–1301. DOI 10.1007/s10924-019-01432-z.

33. Ye, F., Ye, Q. F., Guo, X. J., Zhan, H. H., Fang, C. et al. (2019). Investigation of lanthanum trioxypurine with zinc stearate and pentaerythritol as complex thermal stabilizers for poly(vinyl chloride). *Journal of Vinyl and Additive Technology, 25(4),* 347–358. DOI 10.1002/vnl.21702.

34. Gao, X. X., Jiang, P. P., Zhang, Z. M., Li, Z. H., Li, Y. C. et al. (2021). Synthesis of bismaleate pentaerythritol ester and its application as PVC auxiliary heat stabilizer. *Journal of Applied Polymer Science, 139(12),* 51820. DOI 10.1002/app.51820.

35. Lieberzeit, P., Bekchanov, D., Mukhamediev, M. (2022). Polyvinyl chloride modifications, properties, and applications: Review. *Polymers for Advanced Technologies, 33(6),* 1809–1820. DOI 10.1002/pat.5656.

36. Li, M., Deng, T. X., Ding, H. Y., Yao, N., Xu, L. N. et al. (2022). Preparation and thermal stability of bio-based Na/Zn composite liquid stabilizers for poly(vinyl chloride). *Polymer Degradation and Stability, 201(21),* 109998. DOI 10.1016/j.polymdegradstab.2022.109998.

Supplementary Files

Characterization and Analysis

The Fourier transform infrared (FT-IR) spectra were obtained on a Nicolet iS10 FT-IR (Nicolet Instrument Crop., USA) infrared spectrophotometer. The experiment was performed within 400–4000 cm^{-1} with KBr as a reference.

[1]H nuclear magnetic resonance (^{1}H NMR) was investigated on a Bruker 600 MHz spectrometer (Bruker Instrument Crop., Germany). CDCl$_3$ was used as solvent and tetrametnylsilane (TMS) was used as internal standard in the process.

Weight-average molecular weight was investigated on Agilent 1260 HPLC system with a G7110B pump and a G7162A refractive index detector using HPLC-grade N, N-Dimethylformamide (DMF) as solvent.

The glass transition temperature (T_g) of PVC films was investigated using an American TA Q2000 differential scanning calorimetry (DSC) 200 PC analyzer under N_2 atmosphere. The temperature ranged from −40°C to 120°C at a heating of 10 °C/min.

The thermal stability of prepared PVC samples was determined by Congo red test and discoloration test. The static thermal stability time (T_s) could be obtained by heating the PVC film on a heat stability tester at 180°C according to the standard ISO 182-1–1990. The thermal aging test of the PVC sheet (20 mm × 20 mm pieces) was tested at 180°C according to the ISO 305:1990(E) standard.

The thermogravimetric analysis (TGA) and differential thermal analysis (DTG) was together performed on an American TGA5500 instrument with a heating rate of 10 °C/min from 30°C to 600°C under nitrogen (100 mL/min).

The thermodegradation kinetics of PVC samples were studied using Doyle's method. The samples were analysed by TGA non-isothermal procedure from 30°C to 600°C at multiple heating rates of 5°C, 10°C, 15°C, and 20 °C/min. The nitrogen flow rate was fixed at 100 mL/min. The kinetic parameters such as activation energy (E_a, kJ·mol^{-1}) of the decomposition process was estimated using the equation as shown in Eq. (2).

$$\frac{d\alpha}{dT_\alpha} = \frac{A}{\beta} e^{-E\alpha/RT_\alpha}(1-\alpha)^n \tag{1}$$

$$\frac{d\alpha}{(1-\alpha)^n} = \frac{A}{\beta} e^{-E\alpha/RT\alpha} dT\alpha \tag{2}$$

$$F(\alpha) = \int_0^\alpha \frac{d\alpha}{(1-\alpha)^n} = \int_0^{T\alpha} \frac{A}{\beta} e^{-E\alpha/RT\alpha} dT\alpha \tag{3}$$

$$\lg \beta = \lg[\frac{AE\alpha}{RF(\alpha)}] - 2.315 - 0.4567\frac{E\alpha}{RT\alpha} \tag{4}$$

where β means the heating rate, R represents universal gas constant (8.314 J mol^{-1}K), $F(\alpha) = \int_0^\alpha \frac{d\alpha}{f(\alpha)} = \int_0^\alpha \frac{d\alpha}{(1-\alpha)^n}$. A is apparent pre-exponential factor (s^{-1}). T_α (K) is the temperature when the weight loss α is 20% or 80%. Eq. (4) indicates that lgβ and $1/T_\alpha$ are in linear correlation. E_a can be calculated from the slope (M) and intercept (N) on curves of lgβ change $vs.$ $1/T_\alpha$ as shown in Eq. (5).

$$E_\alpha = -M\frac{R}{0.4567} \tag{5}$$

CMT4303 universal test machine (Sans, China) was take to analyze the tensile modulus, tensile strength and elongation at break of PVC sample according to the ASTM D638-03. The cross head speed of machine was 50 mm/min. The regions used in the tensile test sample were 25 mm long, 0.47 mm thick, 3.98 mm wide.

Solvent resistance of PVC films was investigated according to American Society for Testing Materials (ASTM D5227). PVC films after weighting were immersed in petroleum ether, respectively. The test condition was controlled at 23°C ± 2°C and the relative humidity was restricted at 50% ± 5%. After 24 h, the solvent extracted PVC films were dried and reweighed. The weight loss (W_L) was calculated according to the Eq. (6).

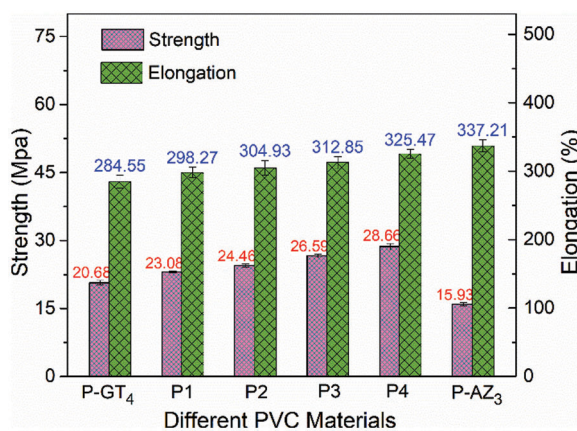$$W_L = \frac{W_1 - W_2}{W_1} \times 100 \tag{6}$$

where W_1 was initial weight of PVC films, and W_2 was final weight of tested PVC films. The extraction loss data was collected using the average value of five test samples.
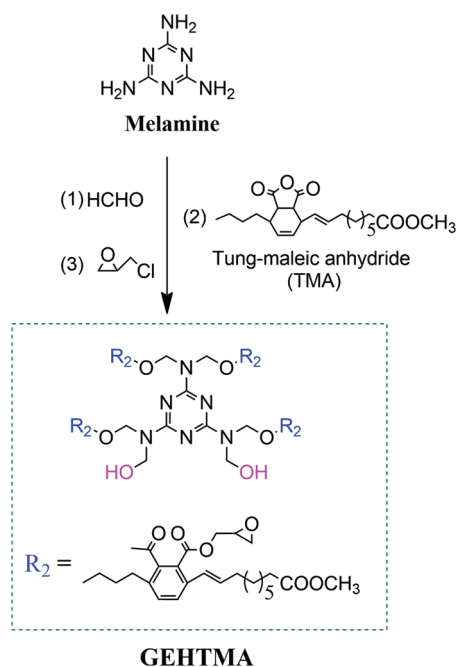
Figure S1: Preparation of hydroxyl, epoxy and nitrogen rich group-containing tung-oil-based ester (GEHTMA-4)

(a)

(b)
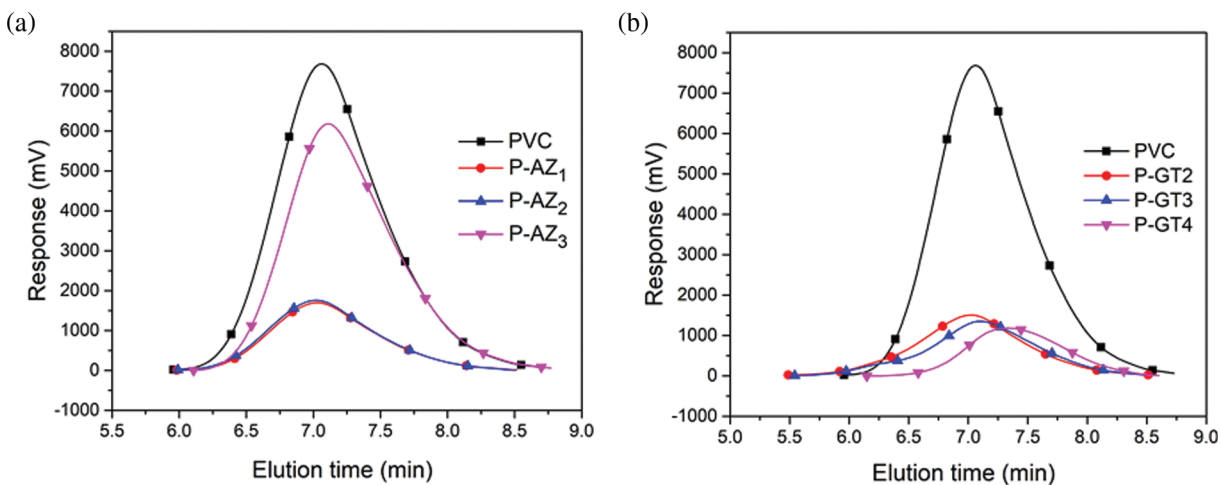
Figure S2: GPC spectra of pure PVC, P-GT$_g$ and P-AZ$_g$

Figure S3: Mechanical properties of P-GT$_4$, P1, P2, P3, P4, and P-AZ$_3$

Table S1: Relative molecular mass and distribution of pure PVC, P-GT$_g$ and P-AZ$_g$

PVC material	Number average molecular weight (M_n, g/mol)	Weight-average molecular weight (M_w, g/mol)	PD (M_w/M_n)
PVC	70738	153004	2.2
P-AZ$_1$	80270	165773	2.1
P-AZ$_2$	83040	172279	2.1
P-AZ$_3$	85738	180122	2.1
P-GT$_2$	87343	199810	2.3
P-GT$_3$	88061	204490	2.3
P-GT$_4$	90183	210187	2.3

Table S2: Values of characteristic from thermogravimetric degradation analysis of PVC/CZ41 and P4

Sample	α/%	β/(°C/min)	T_α/°C
P4	20	5	214.72
		10	229.61
		15	239.39
		20	251.58
	80	5	451.51
		10	464.92
		15	481.92
		20	489.58
CZ41	20	5	224.78
		10	246.59
		15	266.35
		20	276.56
	80	5	415.34
		10	428.71
		15	451.89
		20	457.71